Molecular Therapy
Methods & Clinical Development
Original Article

Inducible caspase-9 suicide gene under control of endogenous oct4 to safeguard mouse and human pluripotent stem cell therapy

Yang Liu,[1,2,3,8] Yang Yang,[4,8] Yangyang Suo,[5] Chuan Li,[2] Min Chen,[2] Shuwen Zheng,[2] Hao Li,[3] Chengcheng Tang,[2] Nana Fan,[3] Ting Lan,[3] Jizeng Zhou,[4] Yingying Li,[3] Jiaowei Wang,[3] Huangyao Chen,[3] Qingjian Zou,[2] and Liangxue Lai[1,2,3,6,7]

[1]School of Life Sciences, University of Science and Technology of China, Hefei 230026, China; [2]Guangdong Provincial Key Laboratory of Large Animal Models for Biomedicine, School of Biotechnology and Health Sciences, Wuyi University, Jiangmen 529020, China; [3]CAS Key Laboratory of Regenerative Biology, Guangdong-Hong Kong Stem Cell and Regenerative Medicine Research Centre, Joint Research Laboratory on Stem Cell and Regenerative Medicine, Guangzhou Institutes of Biomedicine and Health, Chinese Academy of Sciences, Guangzhou 510530, China; [4]School of Biomedical and Pharmaceutical Sciences, Guangdong University of Technology, Guangzhou 510006, China; [5]Joint School of Life Science, Guangzhou Institutes of Biomedicine and Health, Chinese Academic and Sciences, Guangzhou Medical University, Guangzhou 511495, China; [6]Bioland Laboratory (Guangzhou Regenerative Medicine and Health Guangdong Laboratory), Guangzhou 510005, China; [7]Research Unit of Generation of Large Animal Disease Models, Chinese Academy of Medical Sciences (2019RU015), Guangzhou 510530, China

Pluripotent stem cells (PSCs) are promising in regenerative medicine. A major challenge of PSC therapy is the risk of teratoma formation because of the contamination of undifferentiated stem cells. Constitutive promoters or endogenous SOX2 promoters have been used to drive inducible caspase-9 (*iCasp9*) gene expression but cannot specifically eradicate undifferentiated PSCs. Here, we inserted *iCasp9* gene into the endogenous OCT4 locus of human and mouse PSCs without affecting their pluripotency. A chemical inducer of dimerization (CID), AP1903, induced *iCasp9* activation, which led to the apoptosis of specific undifferentiated PSCs *in vitro* and *in vivo*. Differentiated cell lineages survived because of the silence of the endogenous *OCT4* gene. Human and mouse PSCs were controllable when CID was administrated within 2 weeks after PSC injection in immunodeficient mice. However, an interval longer than 2 weeks caused teratoma formation and mouse death because a mass of somatic cells already differentiated from the PSCs. In conclusion, we have developed a specific and efficient PSC suicide system that will be of value in the clinical applications of PSC-based therapy.

INTRODUCTION

Pluripotent stem cells (PSCs) have sustainable self-renewal capabilities. PSCs can differentiate into specific functional cells under appropriate conditions and therefore have been used for cell replacement therapy and organ regeneration.[1,2] However, *in vitro* differentiation may not be entirely complete, and the functional cells are usually mixed with undifferentiated pluripotent cells. The undifferentiated cells may give rise to teratomas when transplanted into recipients and are therefore considered a major safety concern in clinical cell therapy because of their immortal proliferation.[3]

Efforts have been made to reduce tumorigenic risks, including sorting out undifferentiated cells with antibodies that target surface-displayed biomarkers,[4] killing undifferentiated cells with oncolytic virus,[5] or using chemical inhibitors.[6,7] However, these treatments are cumbersome and have untoward side effects. Later, herpes simplex virus thymidine kinase (HSV-TK)-mediated suicide system was used to kill undifferentiated PSCs.[8] HSV-TK reacts with the prodrug ganciclovir (GCV) to be competitively incorporated into the replicated DNA and cause cell death. However, this system can kill only fast-dividing cells. Thus, pluripotent cell populations with slowly dividing capacity are resistant to GCV treatment and remain intact. Unfavorably, GCV has certain liver and kidney toxicity and immunogenicity.[9,10]

Inducible caspase-9 (*iCasp9*) has become a more promising suicide system for pluripotent cell therapy. In the *iCasp9* suicide system, the recruitment area of caspase-9 in the apoptotic pathway is replaced with the dimer binding domain of FK506 binding protein (FKBP12-F36V),[11–13] which ensures caspase-9 dimerization in the presence of a chemical inducer of dimerization (CID), AP1903. The coupled caspase-9 from the induction of CID will activate the downstream signal of caspase-3, which can quickly kill more than 90% of *iCasp9*-expressing cells and even control

Received 21 October 2021; accepted 26 January 2022;
https://doi.org/10.1016/j.omtm.2022.01.014.

[8]These authors contributed equally

Correspondence: Qingjian Zou, Guangdong Provincial Key Laboratory of Large Animal models for Biomedicine, School of Biotechnology and Health Sciences, Wuyi University, Jiangmen 529020, China.
E-mail: wyuchemzqj@126.com
Correspondence: Liangxue Lai, School of Life Sciences, University of Science and Technology of China, Hefei 230026, China.
E-mail: lai_liangxue@gibh.ac.cn

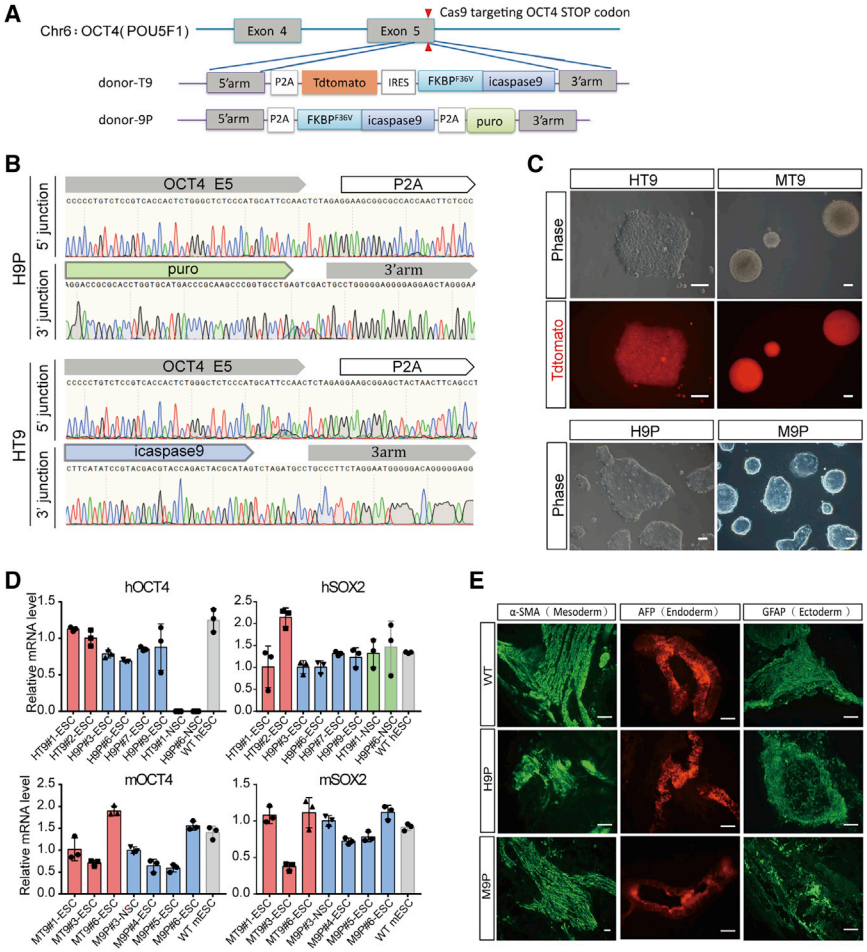

Figure 1. OCT4 gene KI with iCasp9 suicide gene in human and mouse PSCs

(A) Scheme for generating OCT4-iCasp9 clones using CRISPR-Cas9. T9, tdTomato-IRES-iCasp9; 9P, iCasp9-2A-Puro. (B) Sequence analysis of hPSC clones containing the iCasp9 gene in the OCT4 locus confirmed the insertion of the suicide gene. H9P, H9 cell KI with iCasp9-2A-Puro; HT9, H9 cell KI with tdTomato-IRES-iCasp9. (C) Bright-field and fluorescence images of hPSC-iCasp9 and mESC-iCasp9 clones. MT9, 129 mESC KI with tdTomato-IRES-iCasp9; M9P, 129 mESC KI with iCasp9-2A-Puro. Scale bar, 100 μm. (D) Relative mRNA levels of OCT4 and SOX2 in the indicated PSCs. N = 3. Values represent mean ± SD. (E) Immunofluorescence staining of the three germ layer markers of teratomas formed by H9P and M9P cells. Scale bar, 100 μm.

the growth of teratomas in mice.[14–16] However, in these reports, EF1α or other universal promoters were used to drive *iCasp9* gene expression, which could kill all transplanted cells, functional or undifferentiated cells, after CID treatment. The therapeutic effect of functional cells might completely disappear after CID administration.[14,17,18] The use of endogenous pluripotent transcriptional factors to control *iCasp9* gene expression is expected to solve this issue. Previously, SOX2 has been used to control *iCasp9* gene expression in PSCs and induce the suicide of undifferentiated cells by precisely inserting *iCasp9* gene into the downstream of SOX2.[19] SOX2 is a key transcription factor for maintaining pluripotency and a critical regulator of the formation of foregut endoderm and the maintenance of embryonic neural cells and dermal papilla cells.[20,21] Thus, endogenous SOX2 is not an ideal driving factor for the control of the *iCasp9* expression, which specifically induces the suicide of undifferentiated pluripotent cells.

OCT4, one of the most critical factors for pluripotent state maintenance, is expressed specifically in pluripotent cells, including embryonic stem cells, induced PSCs, embryonic germ cells, and cancer stem cells, but not in differentiated cells.[22] The insertion of a fluorescent reporter gene into the OCT4 locus of mouse, human, and porcine PSCs has been used to monitor cell pluripotent state in real time.[23–25] Therefore, in the present study, we inserted the *iCasp9* suicide gene into the downstream of the endogenous OCT4 of human and mouse PSCs. *iCasp9* protein was co-expressed with OCT4 in pluripotent cells, which can induce death through treatment with CID *in vitro* and *in vivo*. Once PSCs are differentiated, CID can no longer affect functional somatic cells. This direct and rapid safety strategy will remarkably reduce the potential risks of the tumorigenesis of PSCs in stem cell therapy.

RESULTS

Knockin (KI) of *iCasp9* suicide gene into the downstream of the OCT4 locus in human and mouse PSCs

iCasp9 was knocked in the downstream of the OCT4 locus to express *iCasp9* in undifferentiated PSCs. A sgRNA targeting a region near the stop codon of the OCT4 locus was designed. Two donor vectors containing tdTomato-IRES-iCasp9 (T9) and iCasp9-2A-Puro (9P) cassettes were designed in frame with human or mouse endogenous *OCT4* genes to prevent the excessive expression of *iCasp9* suicide gene in cells from causing spontaneous cell apoptosis (Figures 1A, S1A, and S1B). TdTomato was used to trace OCT4 expression, and Puro gene encoding Puromycin N-acetyl transferase was used for the convenient screening of targeting cells. Cas9, sgRNA, and the donors were co-transfected into 129 mouse embryonic stem cells (mESCs) and H9 human embryonic stem cells (hESCs). T9 PSC colonies with tdTomato expression were collected by flow cytometry sorting, while 9P PSC colonies were collected under puromycin administration for 7 days. Here, four cell lines of human PSCs inserted

with T9 (named HT9) or 9P (named H9P), as well as mouse PSCs with T9 (named MT9) or 9P (named M9P) were harvested for analysis. The results of agarose gel electrophoresis showed that the expected bands of the PCR products were achieved (Figure S1C). Sequencing the PCR products confirmed that the exogenous genes were precisely inserted into the OCT4 loci (Figures 1B and S1D). To further investigate whether both alleles were integrated with *iCasp9* gene, primers were designed to target 5′ AND-3′ arms, respectively (Figure S1E). A 707-bp band for the wild-type (WT) hESC genome and a 1300-bp band for WT mESC genome were expected. As shown in Figure S1F, among the 13 clones (M9P#3, 4, 5, 6; MT9 #1, 3, 6; H9P#3, 6, 7, 9; and HT9 #1, 2) tested, 11 clones were monoallelic KI clones (Figure S1E and S1F), while only the M9P#3 and #4 were biallelic KI clones. The OCT4-iCasp9 PSCs exhibited typical morphology of ESC morphology (prime state for hESCs and naive state for mESCs) (Figure 1C) and normal proliferation ability (Figure S2A).

Four representative clones, M9P#6, MT9#1, H9P#6, and HT9#1, were selected for further analysis. qPCR and immunofluorescence (IF) tests showed that both human and mouse OCT4-iCasp9 PSCs expressed pluripotent markers including OCT4, SOX2, and Nanog (Figures 1D, S2B, and S2C), and H9P also expressed TRA-1-81. On the contrary, when the human OCT4-iCasp9 ESC differentiated into neural stem cells (NSCs), only SOX2, a marker also observed in neural cells, was still expressed, and OCT4 and Nanog were silenced (Figures 1D and S2C). qPCR was further used to detect the expression of iCasp9. It showed that iCasp9 mRNA was expressed in all four kinds of OCT4-iCasp9 PSCs, and not in their differentiated NSCs (Figure S2C).

Before *in vivo* use of the OCT4-iCasp9 PSCs, we sequenced potential off-target sites of Cas9/gRNA used for KI and detected no off-targets at all detected 15 sites (Figures S3A and S3B). Then, OCT4-iCasp9 PSCs were injected into immunodeficient mice to generate teratomas. It showed that tissues expressed three germ layers markers, such as α-smooth muscle actin (α-SMA), a-fetoprotein (AFP), and glial fibrillary acidic protein (GFAP) (Figure 1E). These results indicated that the insertion of the *iCasp9* gene into OCT4 loci did not negatively affect the pluripotency and self-renewing capacity of the stem cells.

OCT4-iCasp9 PSCs, but not differentiated cells, are selectively eradicated by CID *in vitro*

To explore the influence of *iCasp9* gene structure and copy number on apoptotic regulation, multiple clones were treated with CID. It showed that nearly all of OCT4-iCasp9 PSC clones were stained positive for both propidium iodide (PI) and annexin V (apoptosis marker) after CID was treated for 72 h (Figure S4A). The working concentration of the drug referred to the previous study.[19] There was not much difference between each group. Further drug sensitivity tests showed that 2 h was sufficient for induction of all H9P PSC death, while it took three to four times for HT9 PSC death. Correspondingly, mouse PSC M9P clones took 1–15 h for death, while MT9 needed 60 h or more to die after CID treatment (Figure S4B). The cell lines with one allelic KI or two alleles resulted in little difference of CID dose-response and time course since both biallelic KI clones (M9P #3 and M9P #4) and monoallelic KI clones (M9P #6) would die in 1–2 h after CID treatment (Figure S4B). It is indicated that iCasp9 gene structure (9P or T9) influenced the sensitivity of human and mouse PSCs on CID.

To verify the specificity of the inducible suicide system on PSCs, we tested the effectiveness of CID with a concentration range of 0–200 nM in inducing the apoptosis of four OCT4-iCasp9 PSCs (M9P#6, MT9#1, H9P#6, and HT9#1). The CID had a little toxic effect on WT human and mouse PSCs. The optimal drug concentration was 10 nM (Figure 2A), in which most cells died within 2 h, and nearly all cells died after 6 h with 9P clones (Figure S5A). The dead cells were stained positive for PI or annexin V (Figure S5B), which are markers that represent the occurrence of cell apoptosis. Up to 98% of M9P and H9P cells died within 2 h after CID treatment, whereas HT9 and MT9 required 6 and 72 h, respectively, for thorough apoptosis (Figure 2B). This result indicates that 9P PSCs are more sensitive than T9 PSCs to CID.

The engineered human and mouse PSCs were randomly differentiated *in vitro* for 1 week to confirm whether the CID induced the apoptosis of specific pluripotent cells. At this time, most cells turned into the spindle- or epithelioid-shaped cells, but a portion of cells still huddled as a ball or bump. For M9P and H9P PSCs treated with CID, the clustered clones gradually became loose and could be stained by PI and Hoechst, whereas the surrounding differentiated cells were only stained with Hoechst (Figure S5C), indicating that the CID induced the apoptosis of pluripotent cells and had less effect on differentiated cells. To further confirm this conjecture, we induced H9P and HT9 PSCs cells into NSCs for 12 days (Figure 2C) using the protocol reported previously.[26] The induced NSCs showed high SOX2 and PAX6 expression levels and negative OCT4, Nanog, and iCasp9 expression as confirmed by qPCR (Figure S2B and S2C and IF staining (Figure 2D and S6A). When both H9P ESCs and H9P NSCs were treated with CID for 2 h, nearly all of the H9P-ESCs shrunk and floated as clusters, while the NSCs, derived from H9P-ESCs, grew normally, sticking on dishes (Figure 2E). Fluorescein isothiocyanate (FITC) showed that up to 90% ESCs stained positive for both 7-amino actinomycin D (7AAD) and annexin V, whereas most of the NSCs were negative for the two apoptosis markers (Figure S6B).

Next, to simulate the PSC cell contamination in the clinic, the tdTomato-positive HT9-ESCs and tdTomato-negative HT9-NSCs were mixed with the ratio 0:100, 10:90, 25:75, 50:50, 80:20, 100:0, and co-cultured for 24 h, followed by CID treatment for 6 h (Figure 2F). Results showed that tdTomato-positive cells floated, to die soon after CID administration, while tdTomato-negative cells grew normally on dishes (Figure S6C). Live cells were collected for flow cytometry analysis, and we found that tdTomato-positive cells had died out from the mixture (Figure S6D).

To further confirm that the apoptosis only occurred on ESCs, but not NSCs after being induced by CID, the 40:60 group was stained with

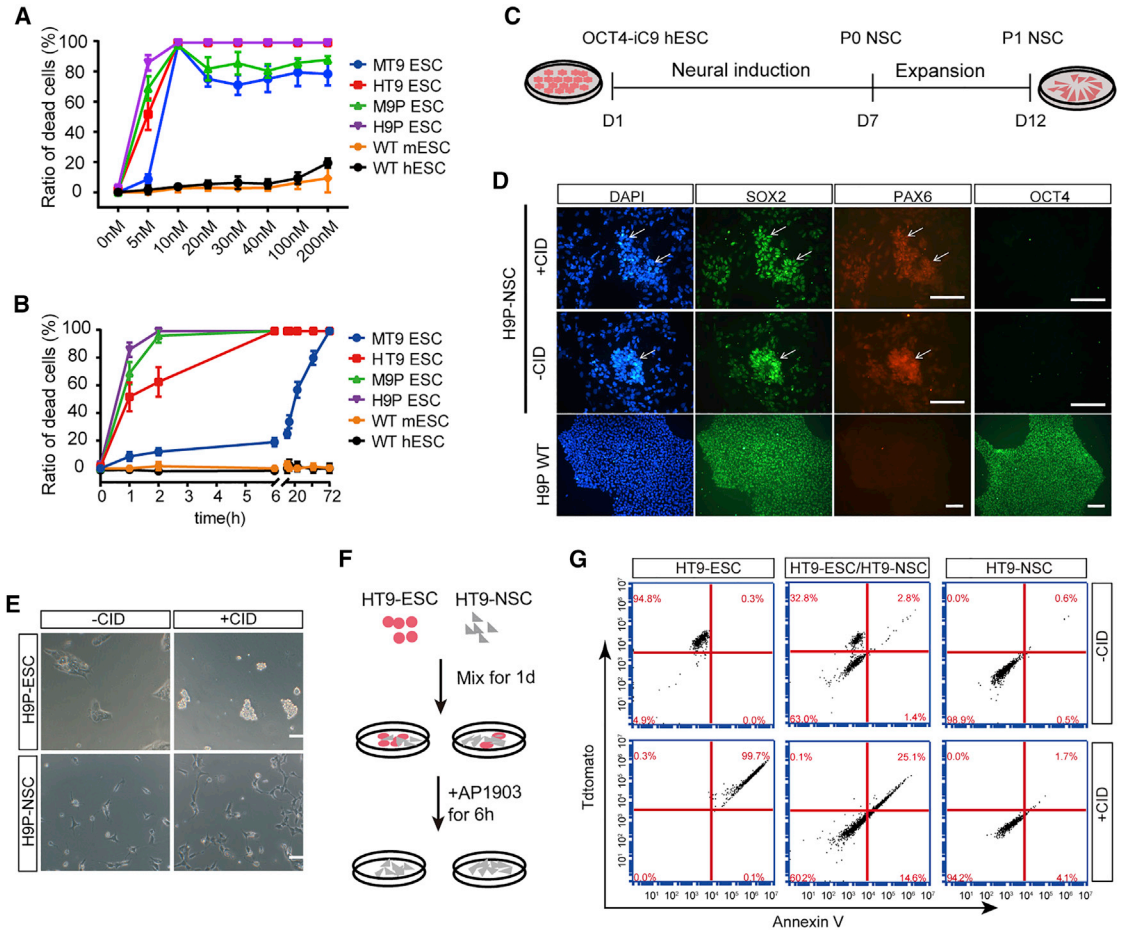

Figure 2. Induced PSC-specific apoptosis of the OCT4-iCasp9 KI system

(A) Effect of AP1903 concentration on OCT4-iCasp9 PSCs by MTS assay. (B) Cell viability of OCT4-iCasp9 PSCs after 10 nM AP1903 treatment at the indicated time as determined by MTS assay. Values represent mean ± SD. (C) Scheme of OCT4-iCasp9 hESCs differentiation to human NSCs. (D) Immunofluorescence staining identification of SOX2, PAX6, and OCT4 in H9P-ESC and H9P-NSC cells with or without AP1903 treatment. Scale bar, 100 μm. (E) Bright-field images of H9P-ESC and H9P-NSC cell after 2 h of treatment with or without 10 nM AP1903 (n = 3). Scale bars, 100 μm. (F) Schematic diagram of CID inducing specific HT9-ESC apoptosis after HT9-ESC and HT9-NSC mixed culture. The culture medium is a 1:1 mixture of both cell culture media. (G) Flow cytometric analysis of HT9-ESC and HT9-NSC cultured in different proportions with or without 10 nM AP1903 (n = 3).

annexin V. Most cells were negatively stained for annexin V. However, when treated with CID, nearly all tdTomato-positive cells were positively stained for annexin V, while tdTomato-negative cells still grew normally (Figures 2G and S6E). These results indicated that the OCT4-iCasp9 inducible system was tightly regulated by CID and enabled to eliminate pluripotent cells, but not differentiated cells.

Mouse OCT4-iCasp9 PSCs are selectively eradicated by CID *in vivo*

M9P cells (2×10^6) were injected subcutaneously into SCID mice to examine the effects of CID treatment on teratoma formation. The CID administration time for each group was set at 2 h before injection (−2h); the same time as M9P cell injection (co-injected); and at days 1, 5, 9, 13, or 17 (marked D1, D5, D9, D13, or D17, respectively) after cell transplantation (Figure S7A). We first used a CID dose of 5 mg/kg to induce apoptosis, but it could hardly inhibit tumor growth. Then, the CID administration dose was increased to 10 mg/kg, and the tumor formation stopped in the D1, D5, D9, and D13 groups (Figure S7B). Thus, 10 mg/kg CID was used in the following experiments.

No teratoma resulted from the injection of OCT4-iCasp9 ESCs in SCID mice when the administration time was −2h, co-injected, D1, and D5 (Figure S7C). The CID administration in these groups resulted in the long-term tumor-free survival of the SCID mice (Figure S7D). In other groups (D9, D13, and D17), teratomas from the injected OCT4-iCasp9 ESCs were observed on D8 and reached 0.8 cm^3 on D9. In the D9 group, the tumor volume gradually became smaller and disappeared on D13 after CID administration. In the D13 group, a tumor with a size of 1.0 cm^3 already developed and also gradually became smaller after CID administration. The tumors in the

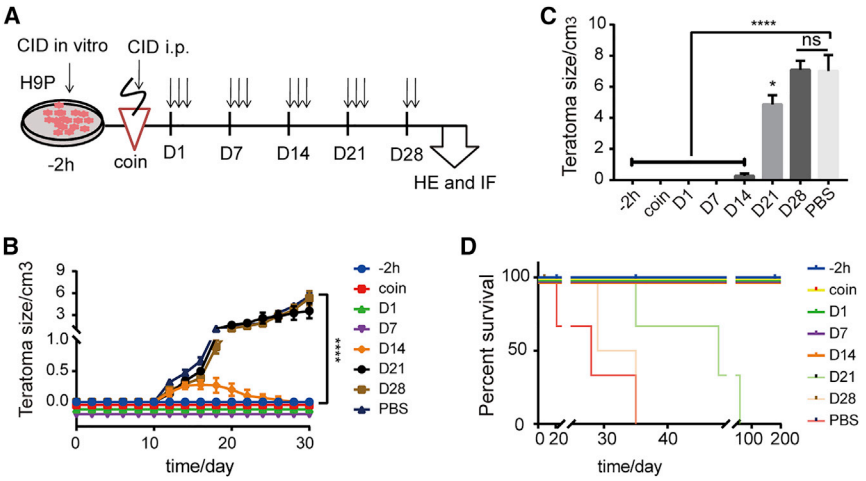

Figure 3. H9P cells are sensitive to CID upon transplantation in mice

(A) Schematic diagram of administration conditions during the construction of teratoma by H9P cells. –2h, administration *in vitro* 2 h before transplantation; coin s.c., co-injection simultaneously; i.p., intraperitoneal administration; D1, the administration group 1 day after transplantation; the other groups are followed by analogy. The arrow represents the times of administration (i.e., 3 consecutive days of administration). (B) Teratoma growth curve. ****$p < 0.0001$, a significant difference between the D21, D28, and PBS groups on D30 and other groups ($n = 3$).

(C) Volume comparison of teratomas formed in different administration groups on D30 ($n = 3$). (D) Survival curves for the eight groups of recipient SCID mice. The mice were euthanized after the tumors reached a diameter greater than 2 cm ($n = 5$).

D17 and PBS groups had a fast growth after D13. The CID had less effect on the development process when applied at D17 (Figure S7D), resulting in mice dying out at D24 (Figure S7E).

Teratoma derived from the D13 group showed an incomplete formation of the germ layers (Figure S7F). By contrast, the teratoma structure of the D17 group, similar to the PBS group, had three distinct germ layers, namely, mesodermal cartilage tissue, endoderm respiratory epithelium, and ectoderm-neuroectoderm characteristic petal-like tissue structure. Moreover, DNA fragmentation as a hallmark feature of apoptosis can be detected by TUNEL staining. The results showed that a large number of cells were stained after CID treatment for 2 days in the tumor from the D13 group. On the contrary, few cells could be stained if the CID was not applied (Figure S7G). We also simultaneously loaded WT mESCs and M9P mESCs by bilateral subcutaneous injection and then intraperitoneally (i.p.) injected CID after 1 week (Figure S7H). After 2 weeks, the volume of tissues from M9P ESCs dramatically decreased compared with the tumor that developed from WT mESCs (Figure S7I). This result indicates that a large number of undifferentiated cells still exist in the teratoma at D13. However, after 17 days, almost all PSCs transformed into various somatic cells.

Human OCT4-iCasp9 ESCs are selectively eradicated by CID *in vivo*

Similar to M9P cells, H9P cells (3×10^6–1×10^7) were also injected subcutaneously into SCID mice. Tumor volumes were monitored every 2 days. Tumor burdens were measured at D35. The CID administration time for each group was set at 2 h before injection (–2h); the same time as H9P cell injection (co-injected); and at day 1, 7, 14, 21, or 28 (marked D1, D7, D14, D21, or D28, respectively) after cell transplantation (Figure 3A). Tumors were observed 12 days after H9P cell injection without the administration of the CID. The tumor volume reached 0.2 cm^3 on D14. When the mice were treated with CID at D14, the tumors stopped growing, and the subsequent tumor volume continued to shrink and finally disappeared on D24. However, when the mice received CID treatment on D21 or D28, the tumor continued to grow similar to that in the control group (Figure 3B). We removed the teratoma tissue on D30 and found that the tumor growth of the D21 group was considerably slower than that of the D28 and PBS groups (Figure 3C). In addition, we also found by observing the survival curves that the mice in the D28 and PBS groups died on D35, whereas the mice in the D21 group survived longer, up to 2 months. The other groups treated with CID before D14 survived for long periods without tumor (Figure 3D). Accordingly, the mortality rate was positively correlated with tumor burden.

To check the OCT4 expression in the teratoma, immunofluorescence was performed to detect OCT4 expression in teratoma. It showed that a large number of H9P ESCs still clustered and expressed OCT4 after being injected for 7 days or 14 days. As time went on, the number of OCT4-positive cells became fewer and fewer, and finally, they disappear on day 28 (Figures 4A and S8). The mice transplanted with the H9P ESCs were treated with CID in the four timings, and then the teratomas were collected. We found that OCT4-positive cells almost disappeared in teratomas achieved in all four timings of CID administration (Figure 4A). Hematoxylin and eosin (H&E) staining demonstrated that the teratoma derived from the D21 group showed a loose structure with three undistinguishable germ layers (Figure 4B). The nucleus of the cell was large and darkly stained with distinct nucleoli, which indicates that some cells had undergone apoptosis. Similar to that injected with PBS, the teratoma from the D28 group contained three distinct germ layers, namely, mesodermal cartilage tissue, endoderm respiratory epithelium, and ectoderm-neuroectoderm characteristic petal-like tissue structure (Figure 4B). TUNEL assay revealed that a large number of cells in tumors from the D21 group were positively stained after CID treatment for 2 days, whereas few cells were positive when CID was not applied (Figure 4C).

We simultaneously loaded WT ESCs and H9P ESCs by bilateral subcutaneous injection and then administered the CID by i.p. injection after 2 weeks. We found that WT ESCs formed a large teratoma

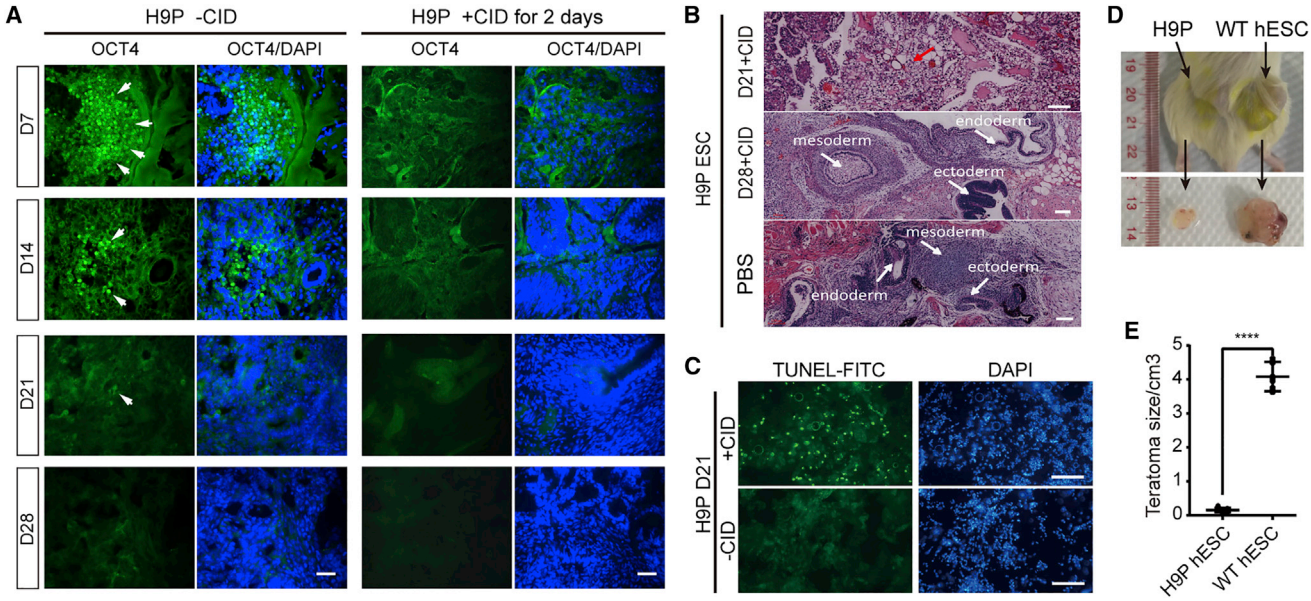

Figure 4. Identification of teratoma from H9P cells after CID administration

(A) Immunostaining of OCT4 from teratoma section after treated with or without CID. Four time points, D7, D14, D21, and D28, were closed for detection. The CID treated groups were stained 2 days after CID administration. Arrows point to the OCT4-positive cells. Scale bar, 50 μm. (B) H&E staining of teratoma in mice at different times treated with CID. Scale bars, 100 μm. The red arrow points to the vacuole area of tissue, and white arrows point to the three germ layers of teratoma. (C) TUNEL staining in the D21 group after being treated with or without CID. Scale bars, 100 μm. (D) Cell transplantation and teratoma formation on D30. H9P and WT hESCs were injected at each side of the mice. (E) Size comparison of teratomas formed by the bilateral subcutaneous injection of WT and H9P PSCs after CID administration (n = 3). Values and error bars reflect the mean ± SD. A major challenge for PSC application is the risk of teratoma formation due to contamination of undifferentiated PSCs. Here, we have constructed the OCT4-iCasp9 safeguard to specifically eliminate undifferentiated tumorigenic cells *in vitro* and *in vivo* by CID (AP1903), which will be of value in clinical applications.

(Figure 4D, right), whereas H9P ESCs turned into a small piece of fat-like soft tissue (Figure 4D, left) after 4 weeks. The volumes of tissue derived from H9P ESCs were much lower than those of tumors from WT ESCs (Figure 4E). These results indicate that CID could specifically kill OCT4-iCasp9 PSCs *in vivo*.

DISCUSSION

In this study, we established KI hESCs and mESCs using the *iCasp9* targeted downstream of endogenous OCT4 promoter. Caspase-9 will form a dimer and start the apoptosis process in pluripotent cells under the control of the CID, AP1903.

Our *in vitro* and *in vivo* test results showed that the specific integration of *iCasp9* into the downstream of OCT4 promoter has no adverse effect on cell proliferation, pluripotency, and differentiation potential, and CID administration could only result in the suicide of pluripotent cells but not differentiated functional cells. Therefore, this method has advantages over similar previous efforts by using the constitutive expression of the suicide gene, which could induce apoptosis in all grafts including both PSCs and differentiated functional cells.

Previous reports showed that the time required for CID-induced suicide is not uniform and varies between 2 and 24 h.[14,15,18,19] Here, we found 9P groups only need 2 h, whereas T9 groups need at least 6 h to specifically induce the apoptosis of pluripotent cells *in vitro*. Internal ribosome entry site (IRES), instead of peptide 2A (P2A), as the upstream of *iCasp9* in T9 groups, might cause less expression of the iCasp9 gene, which would lead to the cells' decreased sensitivity to CID. Biallelic insertion of iCasp9 increased the sensitivity of PSCs to CID compared with correspondingly monoallelic KI cells slightly, although both of them eventually die under CID conditions. Biallelic KI may cause twice the iCasp9 expression, resulting in a faster response to CID, but it may disturb endogenous OCT4 expression. So, monoallelic KI PSCs are more useful cells for pre-clinic therapy.

The formation of the teratomas from H9P cells can be completely controlled by pretreatment of cells with CID 2 h before transplantation or *in vivo* administration with CID within 7 days after transplantation. When H9P cells were allowed to form small tumors in the SCID mice for 2 weeks prior to CID treatment, the formed tumors stopped growing, became smaller, and eventually disappeared in mice, probably because the teratoma was in the premature stage and most cells in the teratoma did not become terminal-differentiated cells.[27] When the mice were treated with CID after 3 weeks, tumors continued to grow similar to those in the PBS group. The mice in the D28 and PBS groups died out at D35, whereas mice in the D21 group had slower tumor growth, lived much longer, but still died out after 2 months. These results indicate that once the transplanted cells formed matured teratoma, CID administration could no longer prevent the impairment caused by tumors in recipients.

OCT4 is the most important transcription factor involved in regulating the self-renewal of ESCs and maintaining pluripotency.[28] OCT4 is also widely expressed in a variety of germline cells and cancer stem cells.[29,30] Therefore, controlling the expression of the suicide gene through OCT4 can be used to kill undifferentiated pluripotent cells, which is the major safety concern for the application of ESCs. However, for iPSC, insertion of exogenous transcript genes into the undesired sites of the genome may cause cancer cells or tumors without expression of OCT4, which would be unable to drive effective iCasp9 expression. This additional safety concern for the iPSC application is out of control by our suicide system. MYC, one of the oncogenes, has been used as a target for inhibition of PSC tumorigenesis.[31] When MYC was blocked by tamoxifen in aggressive PSC-derived cells, the risk of cancer was greatly reduced. However, only 50% of PSCs can be induced apoptosis. Controlling the growth of the tumor requires constant administration of tamoxifen, which is not an ideal solution to address the concern of tumorigenesis. To completely kill these cancer cells, more cancer-specific genes need to be identified to serve as the drivers for specific induction of apoptosis.

In summary, ESCs with *iCasp9* regulated by endogenous OCT4 promotor could be induced to suicide quickly and specifically by the CID, AP1903, *in vitro* and *in vivo*. This method can be used to remove undifferentiated tumorigenic cells before transplantation or to eliminate tumors in the early stages of teratoma formation while keeping the transplanted differentiated cells in function. Therefore, we provided an effective strategy to solve the safety concern of stem cell therapy in clinical practice.

MATERIALS AND METHODS

Ethics statement

SCID immunodeficient mice were purchased from Beijing Vital River Laboratory Animal Technology (Beijing, China) and housed in a specific pathogen-free environment. All animal care and experimental procedures were approved by the Ethical Committee on Animal Experiments at Guangzhou Institutes of Biomedicine and Health, Chinese Academy of Sciences.

Cell culture

Human embryonic stem cells (H9) were cultured using mTeSR (STEMCELL Technologies, Cat. No. 05850). During the passage, Accutase (STEMCELL Technologies) was used to dissociate the cells, and 5 μM Y-27632 (Selleck Chemicals) was added to the culture medium to reduce apoptosis. H9P ESCs formed NSCs by using the PSC Neural Induction Medium (Gibco, Cat. No. A1647801) according to the manufacturer's instructions. The medium used for the mixed culture of HT9-ESC and HT9-NSC is a 1:1 mixture of the two cell culture media.

129 mESCs were cultured in mESC medium, which consisted of high-glucose Dulbecco's modified Eagle's medium (DMEM; Hyclone, South Logan, UT, USA) supplemented with N2 (Gibco, 100X), B27 (Gibco, 50X), 0.1 mmol/L β-mercaptoethanol (Sigma, St. Louis, MO, USA), non-essential amino acids (Gibco, 100X), Glutamax (Gibco, 100X), 1,000 IU/mL leukemia inhibitory factor (Millipore, Billerica, MA), 3 mM CHIR99021 (Stemgent, Beltsville, MD, USA), and 1 mM PD0325901 (Stemgent). Differentiated cells were obtained by culturing in differentiation medium (10% FBS, Gibco; 90% high-glucose DMEM) for 1 week.

All cells were cultured and maintained in a Matrigel-coated (Corning, Cat. No. 356234) plate in an incubator with 5% CO2 at 37°C. The medium was changed every day, and mESCs were passaged every 3–4 days using trypsin-ethylene diamine tetraacetic acid (Gibco, 0.05%). All experiments used cells before the 20th passage and tested for mycoplasma every 2 weeks.

Vector construction

CRISPR plasmids containing the U6 promoter and single-guide RNA (sgRNA) were generated from pX330-U6-Chimeric_BB-CBh-hSpCas9 (Addgene, 42,230) as previous described.[32] The sgRNA was designed by the CRISPR design tool (http://www.rgenome.net) according to the GN19NGG rules to target the locus adjacent to the OCT4 stop codon. The sgRNA sequence for mouse OCT4 targeting is GGTGCCTCAGTTTGAATGCA, and the sgRNA sequence for human OCT4 targeting is GCACCTCAGTTTGAATGCAT.

We designed two donor plasmids, namely, tdTomato-IRES-iCasp9 (T9) and iCasp9-2A-Puro (9P), to prevent the overexpression of the *iCasp9* suicide gene in cells from triggering spontaneous cell apoptosis. Homologous arms (∼2 kb of each site) were amplified by genomic PCR and cloned into the pUC19 vector (Addgene, 74,677) to generate T9 lines. Subsequently, tdTomato-IRES-iCasp9 sequence was ligated with the FKBPF36V-Casp9 gene and inserted between the right and left arms. The donor 9Ps were made using the T9 targeting vector.

Takara PrimerSTAR Max DNA Polymerase (R045A) was used for PCR amplification during plasmid construction. The DNA fragment was purified with HiPure Gel Pure DNA Mini Kit (Magen, D2111-03) and then recombined into the backbone by ClonExpress MultiS One Step Cloning Kit (Vazyme, C113-01). All experiments strictly followed the manufacturer's protocol.

Generation of iCasp9-PSC cells

The transfection of the CRISPR and donor plasmids into hESCs and mESCs was performed using Lipofectamine 3,000 (Life Technologies) following the manufacturer's guidelines. For each targeting, 1 μg gRNA-Cas9 and 2 μg donor plasmids were used for a 6-well plate. Lipofectamine 3,000 and plasmids were separately diluted in Opti-MEM (Life Technologies), mixed and incubated at room temperature for 15 min, and then added dropwise to the medium that was changed in advance. The next day, the 9P group was digested and then diluted in a certain proportion to a 10-cm dish. After 3 days, the 9P group was added with puromycin at a working concentration of 2 μg/mL for 1 week, and then clones were selected for genotype identification. For the T9 group, flow sorting was performed 3 days after transfection

to obtain tdTomato-positive cells, and genotype identification was performed after the clones were formed.

DNA extraction and genotyping

Cells were lysed in 10 μL of lysis buffer (0.45% NP-40 plus 0.6% proteinase K) at 56°C for 60 min and then at 95°C for 15 min. Then, PCR amplification was performed using the cell lysate as the template. The target sequence was amplified from the genome by PCR with specific primers (Table S1). PCR was performed with 37 cycles at 98°C for 15 s, 56°C for 30 s, and 72°C for 30 s by 2× Rapid Taq Master Mix (Vazyme, P222-01). The PCR products were identified by 1.5% agarose gel electrophoresis, imaged with ChemiDoc imaging System, and then sent to Sanger for sequencing (IGE, Guangzhou, China).

Cell viability assay and proliferation rate detection

The cells to be tested (~5,000/well) were collected, mixed with 100 μL of medium, and added to a 96-well plate. The next day, different doses or time gradient administration groups were set, and each plate set had a Control well 1 (only added with 100 μL of medium), Blank well (medium and MTS solution, no cells), and Control well 2 (no drug medium and MTS solution, with cells). CellTiter 96 AQueous One Solution kit (Promega, Madison, MI) was used according to the manufacturer's instructions to test the survival ratio of the cells by MTS analysis.

Cells were seeded into 24-well plates at a density of 1×10^4 per well as the initial cell mass. hESCs were digested into single cells every 2 days and counted with a hemocytometer, whereas mESCs were counted in the same way every other day.

Apoptosis detection and flow cytometry analysis

Apoptosis and Necrosis Assay Kit (Beyotime, C1056) was used for apoptosis detection in M9P and H9P differentiated cells *in situ* according to the manufacturer's instructions. In short, after apoptosis was induced with the CID (AP1903, DC Chemicals), cells in a 24-well plate were stained with cell staining buffer, Hoechst 33,342, and PI solution at 4°C for 20 min. After staining, the cells were washed with PBS once and then observed under a fluorescence microscope.

Annexin V–FITC/PI Apoptosis Detection Kit (Vazyme, A211-01) was used for the *in situ* apoptosis detection of HT9 differentiated cells, and the flow cytometry detection of M9P and H9P cells was in strict accordance with the manufacturer's instructions. The percentage of annexin V−/PI− cells were quantified as live cells, whereas annexin V+/PI− and annexin V+/PI+ cells represent early and late apoptotic cells, respectively.

The H9P and H9P-NSC cells exposed to 10 nM CID for 2 h were harvested and stained with annexin V and 7-AAD according to the manufacturer's instruction (Annexin V:PE Apoptosis Detection Kit I, BD Pharmingen). The detection principle was similar to annexin V/PI; that is, the percentage of annexin V−/7AAD− cells were quantified as live cells. The stained sample was detected by flow cytometry within 1 h. The data for fluorescence-activated cell sorting were collected using an Accuri C6 Plus Flow Cytometer (BD Biosciences).

Off-target analysis

The potential off-target sites of each sgRNA were predicted in human genome to analyze site-specific edits via an online design tool (http://www.rgenome.net/cas-offinder/). All sites were amplified by PCR and then sequenced in Sanger to confirm the off-target effects. All sites and their primers are listed in Table S2.

Real-time quantitative PCR

Total RNA was extracted by using TRIzol reagent (Tiangen, Beijing, China). RevertAid First Strand cDNA Synthesis Kit (Thermo Scientific, K1622) was used for first-strand cDNA synthesis. Real-time PCR was carried out in the CFX96 Touch™ Real-time PCR Detection System (Bio-Rad) using TaKaRa TB Green Premix Ex Taq II (Tli RNaseH Plus, TaKaRa, RR820A). The relative gene expression was normalized to the amount of human GAPDH or mouse β-tubulin mRNA. All experiments were performed in accordance with the manufacturer's instructions, and each gene testing was repeated three times. All genes and their primers are listed in Table S3.

Teratoma formation

The PSCs were counted as 5×10^6 per tube, centrifuged to remove the supernatant, and resuspended in 100 μL of mTeSR and 20 μM ROCK inhibitor Y-27632A. Then, 100 μL of Matrigel (Corning) was quickly added to the cell suspension, and the cell mixture was injected subcutaneously into the subcutis of the dorsal flank of the SCID mice. Tumor size was measured using a vernier caliper every 2 days; the size was calculated using the formula: length × width × height, and survival was recorded. Mice were administered with the CID (5 or 10 mg/kg, i.p.) at different time points once daily for 3 days. The co-injection group received CID and cells by subcutaneous injection during transplantation. Control mice were injected with PBS.

The mice were euthanized when the tumors reached a diameter greater than 2 cm or at 28 weeks of observation. The injection site was examined, and tumor tissues were collected (if present).

Histological analysis

Engraftments were fixed in 4% PFA. After fixation, the engraftments were embedded in optimal cutting temperature compound (OCT) or paraffin for immunofluorescence staining and H&E staining, respectively. The sections were examined and the images were captured on microscope (Motlcampro 285A). TUNEL (TdT mediated dUTP nick end labeling) Apoptosis Detection Kit (FITC) (Yeasen, 40306ES20) was used to detect the nuclear DNA fragmentation characteristic of teratoma tissue cell apoptosis after 3 consecutive days of administration. All experiments were performed in accordance with the manufacturer's instructions.

Immunofluorescence analysis

Cells for staining were cultured in 24 wells coated with Matrigel. Tissues embedded in OCT (Sakura Finetek, Japan) were cut into 8-um

sections. For immunofluorescence, all samples were fixed with 4% paraformaldehyde at room temperature for 10 min, washed with PBS three times, 10 min each, and blocked in PBS containing 3% BSA (Sigma) and 0.1% Triton X-100 at room temperature for 1 h. Then, the samples were incubated at 4°C overnight with the following primary antibodies: Nanog antibody (1:200, AF1977; R&D), SOX2 antibody (1:400, MAB2018; R&D), OCT4 antibody (1:200, sc-5279; Santa Cruz Biotechnology), TRA-1-81 antibody (1:500, MAB4381; Millipore), PAX6 antibody (1:400, Rb901301; Biolegend), α-SMA antibody (1:50, sc-53142; Santa Cruz Biotechnology), AFP antibody (1:50, sc-8399; Santa Cruz Biotechnology), and GFAP antibody (1:50, sc-33673; Santa Cruz Biotechnology). On the second day, the samples were washed three times with PBS and incubated with Alexa Fluor dye-conjugated secondary antibodies (Abcam) for 1 h. 4,6-Diamidino-2-phenylindole (Sigma) was used to stain the nuclei.

Statistical analyses

The GraphPad Prism software (version 8) was used for data analysis. The data are presented as mean ± standard deviation (SD). All tests conducted were individual Student's t tests (*$p < 0.05$, **$p < 0.01$, ***$p < 0.001$, ****$p < 0.0001$, ns: no significance). The number of repetitions of the experiment is indicated in the figure legend.

SUPPLEMENTAL INFORMATION

Supplemental information can be found online at https://doi.org/10.1016/j.omtm.2022.01.014.

ACKNOWLEDGMENTS

This study was supported by the National Key Research and Development Program of China Stem Cell and Translational Research (2017YFA0105103), the Strategic Priority Research Program of the Chinese Academy of Sciences (XDA16030503), the Science Foundation for Young Teachers of Wuyi University (2019TD05), the Key Research & Development Program of Bioland Laboratory (Guangzhou Regenerative Medicine and Health Guangdong Laboratory) (2018GZR110104004), the Science and Technology Planning Project of Guangdong Province, China (2019A030317010, 2017B020231001, 2021B1212040016), the Science and Technology Program of Guangzhou, China (202007030003), the National Natural Science Foundation of China (82001974), the Natural Science Foundation of Guangdong Province of China (2019A1515110283), and the Research Unit of Generation of Large Animal Disease Models, Chinese Academy of Medical Sciences (2019-I2M-5–025).

AUTHOR CONTRIBUTIONS

Y. L. (Yang Liu) and Y. Y. designed and performed most of the experiments. Y. S. and C. L. conducted the animal experiment analysis. M. C., S. Z., H. L., C. T., N. F., T. L., J. Z., Y. L. (Yingying Li), J. W., and H. C. provided technical assistance. Y. L. (Yang Liu) and Q. Z. wrote the manuscript. Q. Z. conceived and supervised the project. L. L. reviewed and edited the manuscript.

DECLARATION OF INTEREST

The authors declare no competing interests.

REFERENCES

1. Lee, J., Rabbani, C.C., Gao, H., Steinhart, M.R., Woodruff, B.M., Pflum, Z.E., Kim, A., Heller, S., Liu, Y., Shipchandler, T.Z., and Koehler, K.R. (2020). Hair-bearing human skin generated entirely from pluripotent stem cells. Nature *582*, 399–404. https://doi.org/10.1038/s41586-020-2352-3.

2. Schwartz, S.D., Regillo, C.D., Lam, B.L., Eliott, D., Rosenfeld, P.J., Gregori, N.Z., Hubschman, J.P., Davis, J.L., Heilwell, G., Spirn, M., et al. (2015). Human embryonic stem cell-derived retinal pigment epithelium in patients with age-related macular degeneration and Stargardt's macular dystrophy: follow-up of two open-label phase 1/2 studies. Lancet *385*, 509–516. https://doi.org/10.1016/S0140-6736(14)61376-3.

3. Nori, S., Okada, Y., Nishimura, S., Sasaki, T., Itakura, G., Kobayashi, Y., Renault-Mihara, F., Shimizu, A., Koya, I., Yoshida, R., et al. (2015). Long-term safety issues of iPSC-based cell therapy in a spinal cord injury model: oncogenic transformation with epithelial-mesenchymal transition. Stem Cell Rep. *4*, 360–373. https://doi.org/10.1016/j.stemcr.2015.01.006.

4. Tang, C., Lee, A.S., Volkmer, J.P., Sahoo, D., Nag, D., Mosley, A.R., Inlay, M.A., Ardehali, R., Chavez, S.L., Pera, R.R., et al. (2011). An antibody against SSEA-5 glycan on human pluripotent stem cells enables removal of teratoma-forming cells. Nat. Biotechnol. *29*, 829–834. https://doi.org/10.1038/nbt.1947.

5. Nagano, S., Oshika, H., Fujiwara, H., Komiya, S., and Kosai, K. (2005). An efficient construction of conditionally replicating adenoviruses that target tumor cells with multiple factors. Gene Ther. *12*, 1385–1393. https://doi.org/10.1038/sj.gt.3302540.

6. Lee, M.O., Moon, S.H., Jeong, H.C., Yi, J.Y., Lee, T.H., Shim, S.H., Rhee, Y.H., Lee, S.H., Oh, S.J., Lee, M.Y., et al. (2013). Inhibition of pluripotent stem cell-derived teratoma formation by small molecules. Proc. Natl. Acad. Sci. U S A *110*, E3281–E3290. https://doi.org/10.1073/pnas.1303669110.

7. Ben-David, U., Gan, Q.F., Golan-Lev, T., Arora, P., Yanuka, O., Oren, Y.S., Leikin-Frenkel, A., Graf, M., Garippa, R., Boehringer, M., et al. (2013). Selective elimination of human pluripotent stem cells by an oleate synthesis inhibitor discovered in a high-throughput screen. Cell Stem Cell *12*, 167–179. https://doi.org/10.1016/j.stem.2012.11.015.

8. Liang, Q., Monetti, C., Shutova, M.V., Neely, E.J., Hacibekiroglu, S., Yang, H., Kim, C., Zhang, P., Li, C., Nagy, K., et al. (2018). Linking a cell-division gene and a suicide gene to define and improve cell therapy safety. Nature *563*, 701–704. https://doi.org/10.1038/s41586-018-0733-7.

9. Traversari, C., Marktel, S., Magnani, Z., Mangia, P., Russo, V., Ciceri, F., Bonini, C., and Bordignon, C. (2007). The potential immunogenicity of the TK suicide gene does not prevent full clinical benefit associated with the use of TK-transduced donor lymphocytes in HSCT for hematologic malignancies. Blood *109*, 4708–4715. https://doi.org/10.1182/blood-2006-04-015230.

10. Berger, C., Flowers, M.E., Warren, E.H., and Riddell, S.R. (2006). Analysis of transgene-specific immune responses that limit the *in vivo* persistence of adoptively transferred HSV-TK-modified donor T cells after allogeneic hematopoietic cell transplantation. Blood *107*, 2294–2302. https://doi.org/10.1182/blood-2005-08-3503.

11. Zhou, X., Naik, S., Dakhova, O., Dotti, G., Heslop, H.E., and Brenner, M.K. (2016). Serial activation of the inducible caspase 9 safety switch after human stem cell transplantation. Mol. Ther. *24*, 823–831. https://doi.org/10.1038/mt.2015.234.

12. Straathof, K.C., Pule, M.A., Yotnda, P., Dotti, G., Vanin, E.F., Brenner, M.K., Heslop, H.E., Spencer, D.M., and Rooney, C.M. (2005). An inducible caspase 9 safety switch for T-cell therapy. Blood *105*, 4247–4254. https://doi.org/10.1182/blood-2004-11-4564.

13. Di Stasi, A., Tey, S.K., Dotti, G., Fujita, Y., Kennedy-Nasser, A., Martinez, C., Straathof, K., Liu, E., Durett, A.G., Grilley, B., et al. (2011). Inducible apoptosis as a safety switch for adoptive cell therapy. N. Engl. J. Med. *365*, 1673–1683. https://doi.org/10.1056/NEJMoa1106152.

14. Yagyu, S., Hoyos, V., Del Bufalo, F., and Brenner, M.K. (2015). An inducible caspase-9 suicide gene to improve the safety of therapy using human induced pluripotent stem cells. Mol. Ther. *23*, 1475–1485. https://doi.org/10.1038/mt.2015.100.

15. Wu, C., Hong, S.G., Winkler, T., Spencer, D.M., Jares, A., Ichwan, B., Nicolae, A., Guo, V., Larochelle, A., and Dunbar, C.E. (2014). Development of an inducible caspase-9 safety switch for pluripotent stem cell-based therapies. Mol. Ther. Methods Clin. Dev. *1*, 14053. https://doi.org/10.1038/mtm.2014.53.

16. Itakura, G., Kawabata, S., Ando, M., Nishiyama, Y., Sugai, K., Ozaki, M., Iida, T., Ookubo, T., Kojima, K., Kashiwagi, R., et al. (2017). Fail-safe system against potential tumorigenicity after transplantation of iPSC derivatives. Stem Cell Rep. *8*, 673–684. https://doi.org/10.1016/j.stemcr.2017.02.003.

17. Nishimura, T., Xu, H., Iwasaki, M., Karigane, D., Saavedra, B., Takahashi, Y., Suchy, F.P., Monobe, S., Martin, R.M., Ohtaka, M., et al. (2019). Sufficiency for inducible Caspase-9 safety switch in human pluripotent stem cells and disease cells. Gene Ther. *27*, 525–534. https://doi.org/10.1038/s41434-020-0179-z.

18. Shi, Z.D., Tchao, J., Wu, L., and Carman, A.J. (2020). Precision installation of a highly efficient suicide gene safety switch in human induced pluripotent stem cells. Stem Cells Transl. Med. *9*, 1378–1388. https://doi.org/10.1002/sctm.20-0007.

19. Wu, Y., Chang, T., Long, Y., Huang, H., Kandeel, F., and Yee, J.K. (2019). Using gene editing to establish a safeguard system for pluripotent stem-cell-based therapies. iScience *22*, 409–422. https://doi.org/10.1016/j.isci.2019.11.038.

20. Hagey, D.W., Klum, S., Kurtsdotter, I., Zaouter, C., Topcic, D., Andersson, O., Bergsland, M., and Muhr, J. (2018). SOX2 regulates common and specific stem cell features in the CNS and endoderm derived organs. PLoS Genet. *14*, e1007224. https://doi.org/10.1371/journal.pgen.1007224.

21. Driskell, R.R., Giangreco, A., Jensen, K.B., Mulder, K.W., and Watt, F.M. (2009). SOX2-positive dermal papilla cells specify hair follicle type in mammalian epidermis. Development *136*, 2815–2823. https://doi.org/10.1242/dev.038620.

22. Suo, G., Han, J., Wang, X., Zhang, J., Zhao, Y., Zhao, Y., and Dai, J. (2005). OCT4 pseudogenes are transcribed in cancers. Biochem. Biophysical Res. Commun. *337*, 1047–1051. https://doi.org/10.1016/j.bbrc.2005.09.157.

23. Lai, S., Wei, S., Zhao, B., Ouyang, Z., Zhang, Q., Fan, N., Liu, Z., Zhao, Y., Yan, Q., Zhou, X., et al. (2016). Generation of knock-in pigs carrying OCT4-tdTomato reporter through CRISPR/Cas9-Mediated genome engineering. PLoS One *11*, e0146562. https://doi.org/10.1371/journal.pone.0146562.

24. Gerrard, L., Zhao, D., Clark, A.J., and Cui, W. (2005). Stably transfected human embryonic stem cell clones express OCT4-specific green fluorescent protein and maintain self-renewal and pluripotency. Stem Cells *23*, 124–133. https://doi.org/10.1634/stemcells.2004-0102.

25. Shi, Y., Desponts, C., Do, J.T., Hahm, H.S., Scholer, H.R., and Ding, S. (2008). Induction of pluripotent stem cells from mouse embryonic fibroblasts by OCT4 and Klf4 with small-molecule compounds. Cell Stem Cell *3*, 568–574. https://doi.org/10.1016/j.stem.2008.10.004.

26. Park, T.S., Zimmerlin, L., Evans-Moses, R., Thomas, J., Huo, J.S., Kanherkar, R., He, A., Ruzgar, N., Grebe, R., Bhutto, I., et al. (2020). Vascular progenitors generated from tankyrase inhibitor-regulated naive diabetic human iPSC potentiate efficient revascularization of ischemic retina. Nat. Commun. *11*, 1195. https://doi.org/10.1038/s41467-020-14764-5.

27. McDonald, D., Wu, Y., Dailamy, A., Tat, J., Parekh, U., Zhao, D., Hu, M., Tipps, A., Zhang, K., and Mali, P. (2020). Defining the teratoma as a model for multi-lineage human development. Cell *183*, 1402–1419.e18. https://doi.org/10.1016/j.cell.2020.10.018.

28. Masui, S., Nakatake, Y., Toyooka, Y., Shimosato, D., Yagi, R., Takahashi, K., Okochi, H., Okuda, A., Matoba, R., Sharov, A.A., et al. (2007). Pluripotency governed by SOX2 via regulation of Oct3/4 expression in mouse embryonic stem cells. Nat. Cell Biol. *9*, 625–635. https://doi.org/10.1038/ncb1589.

29. Mehravar, M., and Poursani, E.M. (2021). Novel variant of OCT4, named OCT4B5, is highly expressed in human pluripotent cells. Stem Cell Rev. Rep. *17*, 1068–1073. https://doi.org/10.1007/s12015-020-10093-8.

30. Koo, B.S., Lee, S.H., Kim, J.M., Huang, S., Kim, S.H., Rho, Y.S., Bae, W.J., Kang, H.J., Kim, Y.S., Moon, J.H., and Lim, Y.C. (2015). OCT4 is a critical regulator of stemness in head and neck squamous carcinoma cells. Oncogene *34*, 2317–2324. https://doi.org/10.1038/onc.2014.174.

31. Oricchio, E., Papapetrou, E.P., Lafaille, F., Ganat, Y.M., Kriks, S., Ortega-Molina, A., Mark, W.H., Teruya-Feldstein, J., Huse, J.T., Reuter, V., et al. (2014). A cell engineering strategy to enhance the safety of stem cell therapies. Cell Rep. *8*, 1677–1685. https://doi.org/10.1016/j.celrep.2014.08.039.

32. Mali, P., Yang, L., Esvelt, K.M., Aach, J., Guell, M., DiCarlo, J.E., Norville, J.E., and Church, G.M. (2013). RNA-guided human genome engineering via Cas9. Science *339*, 823–826. https://doi.org/10.1126/science.1232033.